

High-current dc power transmission in flexible RE–Ba₂Cu₃O_{7– δ} coated conductor cables*

D C van der Laan^{1,2}, L F Goodrich² and T J Haugan³

¹ Department of Physics, University of Colorado, Boulder, CO 80309, USA

² National Institute of Standards and Technology, Boulder, CO 80305, USA

³ Air Force Research Laboratory, Wright-Patterson AFB, OH 45433, USA

E-mail: danko@boulder.nist.gov

Received 9 August 2011, in final form 6 September 2011

Published 1 December 2011

Online at stacks.iop.org/SUST/25/014003

Abstract

Transmission cables made from high-temperature superconductors have been successfully demonstrated within the electric power grid. These cables carry an ac current of up to 3000 A in a much smaller cross-sectional area than conventional transmission lines, but they are not flexible enough for certain applications that involve very tight cable bends. Certain on-board Air Force applications require 5 MW of dc power transmission at 270 V and current of 18 500 A and would benefit from superconducting transmission in lightweight, flexible cables that would be cooled with helium gas down to about 55 K. To address these needs, we have constructed a 10 mm diameter RE–Ba₂Cu₃O_{7– δ} (RE = rare earth) coated conductor cable that is lighter and more flexible than the current generation of superconducting cables, and that has a critical current of 7561 A at 76 K. The cable is expected to have a critical current of more than 20 000 A at 55 K and therefore will likely exceed the requirements for 5 MW on-board power transmission. The cable consists of two electrically insulated phases that can be operated in different modes, which allows us to study the effect of self-field on the cable performance.

1. Introduction

A major effort to develop high-temperature superconductors (HTS) for power-grid applications has resulted in HTS ac power transmission cables that carry up to 3000 A rms per phase and operate at temperatures between 65 and 77 K in liquid nitrogen [1–3]. These cables are constructed from either Bi₂Sr₂Ca₂Cu₃O_x (Bi-2223) tapes, or YBa₂Cu₃O_{7– δ} (YBCO) coated conductors. They are designed to replace existing copper and aluminum cables within the transmission or distributions networks of the electric power grid, thereby decreasing the cable size, while increasing its capacity. The cables are constructed by winding a large number of superconducting tapes around a hollow or solid former that has a relatively large diameter of at least 1.6 cm. The use of a large former has the benefit that a relatively high number of tapes can be wound into a limited number of layers, which ensures an even current distribution at frequencies around

60 Hz. On the other hand, it limits the minimum cable bending diameter and results in a relatively high cable mass. Several Department of Defense applications would benefit from superconducting transmission cables that are lighter and more flexible than the current generation of HTS power transmission cables [4, 5], such as an on-board Air Force dc power transmission cable that carries about 5 MW of power at 270 V and 18 500 A.

We have recently demonstrated the feasibility of constructing flexible high-current superconducting cables from RE–Ba₂Cu₃O_{7– δ} (REBCO) coated conductors using 5.5 mm diameter formers and outer diameter of 7.5 mm [6] that can carry a dc current of as much as 2800 A at 76 K. Here, we show that this particular cable design has great potential for flexible transmission cables that are even smaller and carry more current than conventional HTS cables under dc operating conditions. A cable that is intended to meet the Air Force interest of 18 500 A at 55 K was constructed and tested at 76 K in liquid nitrogen, where it should carry at least 6800 A in a single phase.

* Contribution of NIST, not subject to US copyright.

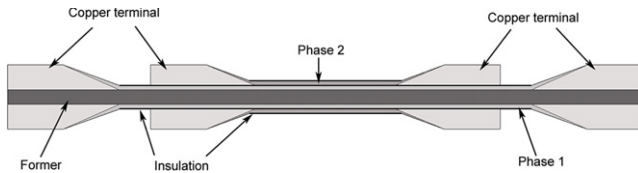


Figure 1. Cross-section of the two-phase cable with copper terminals. Not to scale.

2. The experiment

The REBCO coated conductors used to construct a superconducting cable were produced through the ion-beam-assisted deposition (IBAD), metal–organic chemical-vapor deposition (MOCVD) process on 50 μm thick Hastelloy C-276 substrates [7, 8]. The 4 mm wide coated conductors were surround-plated with 20 μm of copper for electrical stability. Their critical current density at 76 K and self-field was about 3.0 MA cm^{-2} .

The dependence of the critical current (I_c) of the coated conductors on the axial strain (ϵ) was measured at 76 K. The samples were soldered onto the surface of a 98 wt% Cu–2 wt% Be (CuBe) beam. Axial strain was applied by bending the beam in a four-point bender [9], and strain was measured directly with strain gages mounted on top of the beam. The critical currents of single conductors and full cables were determined with a four-contact measurement with an uncertainty of about $\pm 0.5\%$ at an electric field criterion of $1 \mu\text{V cm}^{-1}$.

The cable, about 1 m in length, consisted of two electrical phases that were electrically insulated from each other with polyamide tape (see figure 1). This configuration enabled the testing of the cable with a set of power supplies that was limited to about 5000 A, while the full cable, carrying currents in the two phases running in the same direction, was expected to carry over 6800 A. Both phases were wound into a co-axial configuration, where the coated conductors were spiral-wound around a single insulated copper former that had an outer diameter of 5.5 mm. Each superconducting layer was wound by hand in the direction opposite to the winding direction of its neighboring layer. Four copper current terminals, 6.35 cm in diameter, were soldered to the coated conductors at the ends of the two phases. Voltage contacts were soldered onto some of the coated conductors located in the outer layer of each phase, as well as on the current terminals.

The first electrical phase consisted of 10 layers with a total of 39 coated conductors, and the second phase consisted of 7 layers with a total of 40 coated conductors. The number of tapes per layer increased with cable diameter, as is outlined in table 1. Included in the table are the radius r of each layer, the twist pitch p of the coated conductors in each layer, the total conductor length per layer per meter of cable, the conductor length factor defined as the individual tape length in each layer per meter of cable, and the calculated strain in the superconducting film based on the calculation outlined in [10]. A total of 79 coated conductors were wound into 17 layers. The total coated conductor length per meter of cable was about

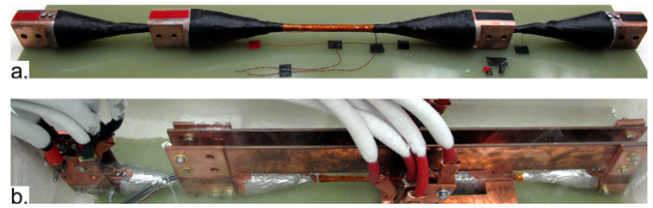


Figure 2. (a) Two-phase, 10 mm diameter, REBCO coated conductor cable. (b) Cable testing in single-phase mode in liquid nitrogen with the two phases connected in series and with the currents running in the same direction.

(This figure is in colour only in the electronic version)

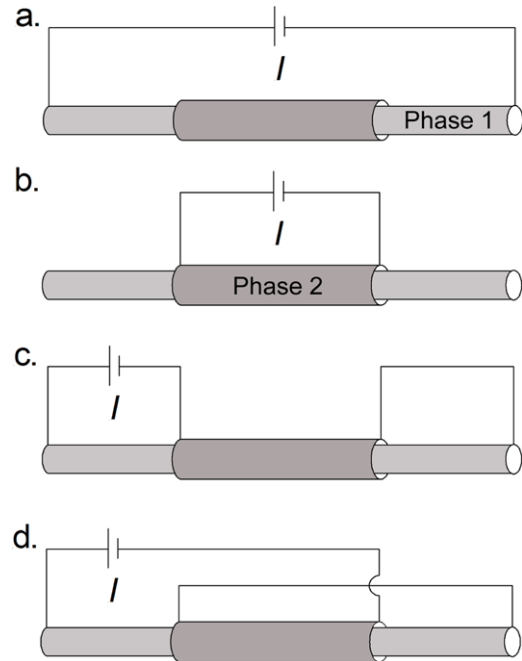


Figure 3. Four different configurations in which the two phases of the cable were tested. (a) Stand-alone configuration for measuring the critical current of phase 1, and (b) the critical current of phase 2. (c) Two-phase configuration in which the two phases were connected in series and the currents in the two phases ran in opposite directions. (d) Single-phase configuration in which the two phases were connected in series and the currents in the two phases ran in the same direction.

105 m. The completed two-phase cable is shown in figure 2(a), and the cable during the single-phase test (see below) is shown in figure 2(b). The cable weight is about 0.44 kg m^{-1} .

The critical current of the cable was measured in different configurations (see figure 3). First, the critical current of each individual phase was measured (figures 3(a) and (b)). Then, the cable was tested as a two-phase cable with the currents in the two phases running in opposite directions (figure 3(c)). Finally, the cable was tested as a single-phase cable with the two phases connected in series and the currents in the two phases running in the same direction. This particular configuration enabled us to test the full cable with our current supplies that were limited to a total current of about 5000 A. The two configurations in which the two phases were connected in series also enabled us to study the effect of self-field on the cable performance.

Table 1. Cable parameters.

Layer	Number of tapes	r (mm)	p (mm)	Meters of tape/ meter of cable	Length factor	ε (%)	Calculated I_c per tape (A)	Calculated layer I_c (A)
Phase 1								
1	3	2.77	30	4.35	1.45	-0.52	108.65	325.95
2	3	2.92	31	4.59	1.53	-0.50	109.71	329.14
3	3	3.07	33	4.82	1.61	-0.47	111.33	333.98
4	3	3.22	34	5.06	1.69	-0.45	112.13	336.38
5	4	3.37	48	5.29	1.32	-0.32	117.90	471.60
6	4	3.52	48	5.53	1.38	-0.33	117.85	471.40
7	4	3.67	48	5.76	1.44	-0.33	117.82	471.29
8	5	3.82	72	6.00	1.20	-0.20	121.72	608.60
9	5	3.97	66	6.24	1.25	-0.23	121.00	605.02
10	5	4.12	68	6.47	1.29	-0.22	121.18	605.88
Phase 2								
11	5	4.20	52	6.60	1.32	-0.30	118.74	593.68
12	5	4.35	54	6.83	1.37	-0.29	119.12	595.61
13	6	4.50	75	7.07	1.18	-0.20	121.73	730.36
14	6	4.65	74	7.30	1.22	-0.21	121.60	729.60
15	6	4.80	66	7.54	1.26	-0.24	120.79	724.73
16	6	4.95	70	7.78	1.30	-0.22	121.18	727.08
17	6	5.10	69	8.01	1.34	-0.23	121.07	726.41

3. Results and discussion

The superconducting layer of a REBCO coated conductor is placed under axial compression when spiral-wound on a round former [10], and because I_c changes reversibly with compressive strain [9], we expect the performance of the conductors in the cable to be different from that of a straight sample. The strain dependence of I_c as a function of compressive strain (see figure 4) was measured for a straight REBCO coated conductor, before cabling, to allow calculating the critical current of the coated conductors in the cable. The strain dependence of I_c was fully reversible up to at least -0.78% compression, which was verified by unloading the strain and measuring I_c again (open symbols). The expected strain range experienced by the conductors in the cable is indicated by the gray area in the figure, which shows that the critical current of the conductors in the cable is expected to be between 87% and 97% of their initial value (see also table 1).

The strain dependence of I_c in REBCO coated conductors is often described with a power-law fitting function [9]:

$$I_c(\varepsilon) = I_c(0)(1 - a|\varepsilon - \varepsilon_m|^{2.18}). \quad (1)$$

The parameter values of the fit shown in figure 4 are: $I_c(0) = 125 \pm 10$ A (the uncertainty is determined by the variation in I_c over the length of the conductor), $a = 9118$, and $\varepsilon_m = 0.09\%$. This expression allows us to calculate the critical current of each REBCO coated conductor in the cable, on the basis of the calculated strain of its superconducting film, which depends on its bending diameter and its twist pitch [10]. The estimated applied strain and I_c for each tape in the cable are listed in table 1, as well as the total estimated I_c for each layer. The expected average I_c of the tapes in the cable is about 118.8 A.

The critical current of the first phase of the cable (phase 1) was measured at 76 K in liquid nitrogen, as shown in

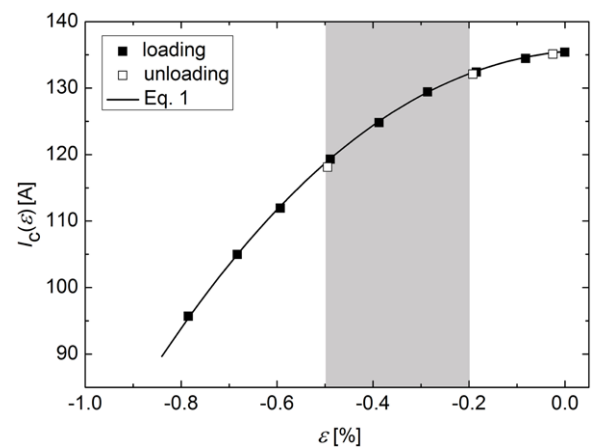


Figure 4. Strain dependence of I_c for one of the REBCO coated conductors before the cable was wound. The critical current under loading is represented by solid symbols, while I_c that was measured after the strain has been unloaded is represented by open symbols. The solid line is equation (1) and the gray area indicates the range of strain of the coated conductors in the cable.

figure 3(a), before phase 2 was wound on top of phase 1. Three sets of voltage taps were soldered onto phase 1; set 1–1 was soldered near the middle of the cable, at a spacing of 15 cm, set 1–2 was soldered near the ends of the cable, at a spacing of 90 cm, and set 1–3 was soldered onto the copper terminals of phase 1. A quench detector was connected to the voltage taps that were soldered to the cable terminals to protect the cable during a possible quench or thermal runaway. The electric fields that were determined with the three sets of voltage contacts are plotted as a function of current in figure 5(a). A sharp superconducting transition was measured with set 1–1, located near the middle of the cable, at a critical current of 3724 A (see table 2). The cable experienced a thermal

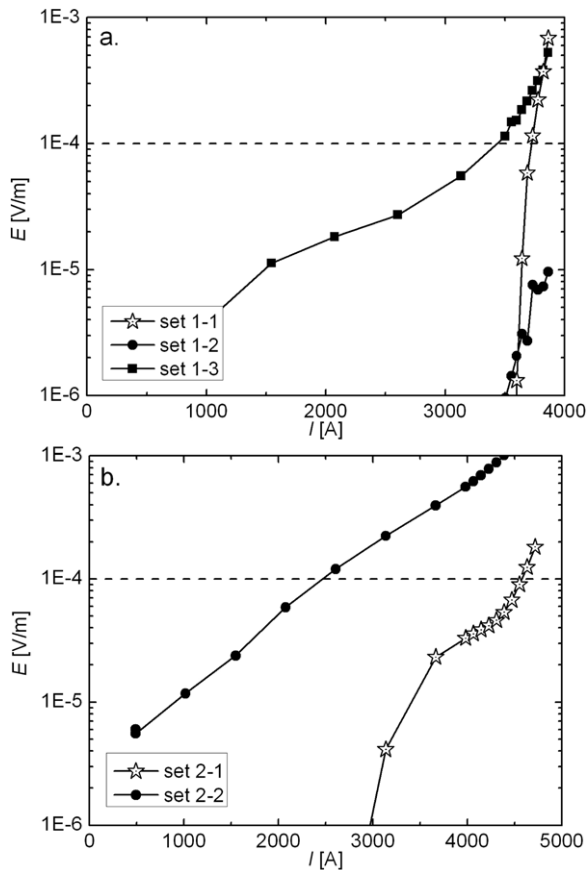


Figure 5. (a) Electric fields as a function of current for cable phase 1. Set 1–1 is the voltage taps located near the middle of the cable, set 1–2 is located near the ends of the cable, and set 1–3 is located on top of the current terminals. (b) Electric fields as a function of current for cable phase 2. Set 2–1 is the voltage taps located near the middle of the cable, and set 2–2 is located on top of the current terminals. The dashed lines indicate the electric field criterion.

runaway at a current above 3863 A, before a superconducting transition could be measured with set 1–2, near the cable ends. A critical current of about 4300 A is estimated by extrapolating the voltage measured with set 1–2 to an electric field of $1 \mu\text{V cm}^{-1}$. The critical currents of phase 1, as determined with sets 1–1 and 1–2, are about 15% and 6% lower than the expected critical current of 4559 A. The expected critical current is the sum of the critical current of the individual coated conductors in the cable, corrected for the reversible decrease in I_c due to the applied compressive strain; it is the summation of the layer I_{cs} of layers 1–10 listed in table 1. A possible variation in I_c along the length of the conductor and a relatively high self-field of about 181 mT on the surface of phase 1, which is calculated by use of Ampère’s law, likely explain the deviation between the measured and the expected I_{cs} .

The critical current of phase 2 of the cable was determined at 76 K, as outlined in figure 3(b), with only one set of voltage taps on the cable, set 2–1, separated by 20 cm. The results are shown in figure 5(b). The overall voltage across phase 2 was measured with a set of voltage taps, set 2–2, that was soldered to the copper terminals to which a quench detector was connected. The critical current of phase 2 is 4600 A, which

Table 2. Measured critical currents of phases 1 and 2.

Mode of operation	Phase	Tap number	I_c (A)	Maximum self-field (mT)
Stand-alone (figure 3(a))	1	1–1	3724	181
		1–2	≈ 4300	210
Stand-alone (figure 3(b))	2	2–1	4600	186
Two-phase (figure 3(c))	1	1–1	3946	192
	2	2–1	(>4600)	
Single-phase (figure 3(d))	1	1–1	3745	183
	2	2–1	3816	302

is only 5% less than the expected I_c (equal to the summation of the layer I_{cs} of layers 11–17 listed in table 1). The difference is expected to be caused, in part, by the self-field, which is 186 mT on the outer surface of phase 2. Phase 2 of the cable did not experience a quench or thermal runaway, but the cable current was limited experimentally to 4716 A. The total critical currents of the two phases operated individually is 8324 A, but the interaction between the two phases is expected to influence the performance of the cable when the two phases are operated simultaneously.

The critical currents of phases 1 and 2 were determined when the cable was operated as a two-phase cable. The two phases were connected in series, with the currents running in opposite directions in the two phases, as shown in figure 3(c). The voltages that were measured as a function of current with set 1–1 on phase 1 and set 2–1 on phase 2 are shown in figures 6(a) and (b), respectively, where they are compared to the voltages measured in both stand-alone tests. A slight increase in critical current was measured for phase 1, where I_c is 3946 A in two-phase operation (see table 2), compared to 3724 A for stand-alone operation. The two phases do not form a solid body, due to the small gaps that exist between the conductors in each layer; thus the slight increase in I_c of phase 1 could potentially be explained by a change in magnetic field distribution near the top layers of phase 1 due to the presence of the second phase with opposing current. The cable experienced a thermal runaway at 3844 A, 100 A below the extrapolated critical current of phase 1, due to heating at one of the current terminals of phase 1.

A higher critical current for phase 2 is expected due to the lower self-field in phase 2 when the magnetic fields of the two phases cancel in this particular configuration. Unfortunately, the critical current of phase 2 could not be determined because of the thermal runaway. The voltage rise measured with voltage contact set 2–1 occurs at a higher current (see figure 6(b)), which indicates that I_c is expected to be higher compared to that for the stand-alone operation of phase 2.

The cable was also operated as a single-phase cable, with the two phases connected in series and with the currents in the two phases running in the same direction. This mode of operation, where the current of phase 1 is looped back into phase 2 outside of the cable, is outlined in figure 3(d). A picture of the cable during testing is shown in figure 2(b). The voltages measured with set 1–1 on phase 1 and set 2–1 on phase 2 are included in figures 6(a) and (b), respectively.

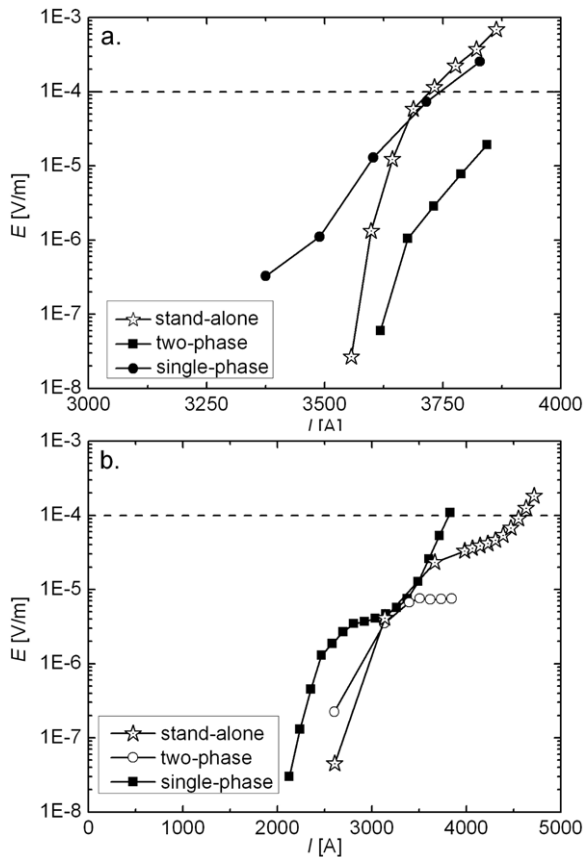


Figure 6. (a) Electric fields as a function of current for cable phase 1 during different modes of operation, determined with voltage contact set 1–1 near the center of phase 1. (b) Electric field as a function of current for cable phase 2 during different modes of operation, determined with voltage contact set 2–1 near the center of phase 2. The modes of operation are stand-alone, two-phase with opposing currents, and single-phase with aligned currents. The dashed lines indicate the electric field criterion.

The critical current of phase 1 of 3745 A is within 0.5% of I_c determined during the stand-alone test of phase 1 (see table 2). On the other hand, the critical current of phase 2 of 3816 A is 17% lower than that of the stand-alone test of phase 2. The reduction in I_c of phase 2 is caused by the much higher self-field of 302 mT at the surface of the cable when the two phases are operated in series with currents running in the same direction. The total critical current of the cable operating in single-phase mode at 76 K is 7561 A. The cable performance results in a mass specific power rating at 270 V m^{-1} of cable of 4.6 MW $kg^{-1} m^{-1}$ at 76 K and of an estimated 12.5 MW $kg^{-1} m^{-1}$ at 55 K, which excludes the cryostat.

The successful testing of the dc power transmission cable, consisting of two electrically insulated co-axially wound phases, demonstrates its capability to carry very large currents in a relatively small cross-section at liquid nitrogen temperatures. The cable critical current of 7561 A at 76 K is expected to be about 15 000 A at 65 K in pumped liquid nitrogen and 20 400 A at 55 K in helium gas. The cable is thus expected to exceed the requirements for the 5 MW dc power

transmission cable for Air Force applications that will operate at 270 V. The effect of the cable self-field on its performance has been demonstrated, where the critical currents of the two stand-alone phases would add up to 8324 A, while the higher self-field decreases the cable performance by about 9% to 7561 A when the two phases are operated simultaneously. The cable could potentially be used in areas other than within the Department of Defense. It could be applicable within the electric power grid at locations where dc power transmission is desired, or within current distribution systems at high-energy physics accelerators.

4. Conclusions

We have constructed a 10 mm diameter, two-phase, dc power transmission cable from REBCO coated conductors having a critical current of 7561 A at 76 K. The cable is expected to exceed the requirements for 5 MW power transmission at 270 V and 18 500 A for certain Air Force applications. The self-field of the cable lowers its critical current by about 9% when the two phases are operated in parallel, compared to the total critical current of 8324 A, when the two phases are operated separately. The highest cable performance is demonstrated when the cable is operated as a two-phase cable with the two phases carrying current in opposite directions, canceling the self-field on the surface of the cable.

Acknowledgments

This work was supported in part by the US Department of Energy, Office of Electricity Delivery and Energy Reliability and the Air Force Research Laboratory. Certain commercial materials are referred to in this paper to foster complete understanding. Such identification implies neither recommendation nor endorsement by NIST, nor that the materials identified are necessarily the best available for the purpose.

References

- [1] Demko J A *et al* 2007 *IEEE Trans. Appl. Supercond.* **17** 2047
- [2] Yumura H, Ashibe Y, Itoh H, Ohya M, Watanabe M, Masuda T and Weber C S 2009 *IEEE Trans. Appl. Supercond.* **19** 1698
- [3] Maguire J F, Yuan J, Romanosky W, Schmidt F, Soika R, Bratt S, Durand F, King C, McNamara J and Welsh T E 2011 *IEEE Trans. Appl. Supercond.* **21** 961
- [4] Haugan T J, Long J D, Hampton L A and Barnes P N 2008 *SAE Int. J. Aerospace* **1** 1088–94
- [5] Fitzpatrick B K, Golda E M and Kephart J T 2008 *Adv. Cryog. Eng.* **53A** 277–83
- [6] van der Laan D C, Lu X F and Goodrich L F 2011 *Supercond. Sci. Technol.* **24** 042001
- [7] Selvamanickam V *et al* 2001 *IEEE Trans. Appl. Supercond.* **11** 3379
- [8] Selvamanickam V, Xie Y, Reeves J and Chen Y 2004 *MRS Bull.* **29** 579
- [9] van der Laan D C and Ekin J W 2007 *Appl. Phys. Lett.* **90** 052506
- [10] van der Laan D C 2009 *Supercond. Sci. Technol.* **22** 065013